Infinite-layer LaNiO$_2$:   Ni^{1+} is not Cu^{2+}

K.-W. Lee and W. E. Pickett

Department of Physics, University of California, Davis, California 95616, USA
(Received 26 May 2004; published 21 October 2004)

The Ni ion in LaNiO$_2$ has the same formal ionic configuration $3d^9$ as does Cu in isostructural CaCuO$_2$, but it is reported to be nonmagnetic and probably metallic whereas CaCuO$_2$ is a magnetic insulator. From *ab initio* calculations we trace its individualistic behavior to (1) reduced $3d$–$2p$ mixing due to an increase of the separation of site energies $(\varepsilon_d-\varepsilon_p)$ of at least 2 eV, and (2) important Ni $3d(3z^2-r^2)$ mixing with La $5d(3z^2-r^2)$ states that leads to Fermi surface pockets of La $5d$ character that hole dope the Ni $3d$ band. Correlation effects do not appear to be large in LaNiO$_2$. However, *ad hoc* increase of the intra-atomic repulsion on the Ni site (using the LDA+U method) is found to lead to a correlated state: (i) the transition metal $d(x^2-y^2)$ and $d(3z^2-r^2)$ states undergo consecutive Mott transitions; (ii) their moments are *antialigned* leading (ideally) to a "singlet" ion in which there are two polarized orbitals; and (iii) mixing of the upper Hubbard $3d(3z^2-r^2)$ band with the La $5d(xy)$ states leaves considerable transition metal $3d$ character in a band pinned to the Fermi level. The magnetic configuration is more indicative of a Ni^{2+} ion in this limit, although the actual charge changes little with U.

I. INTRODUCTION

The perovskite oxide LaNiO$_3$, purportedly an example of a correlated metallic Ni^{3+} system, has been investigated over some decades by a few groups[1–3] for possible exotic behavior. The oxygen-poor lanthanum nickelate LaNiO$_x$ has also attracted attention, because of characteristic changes of its electronic and magnetic properties as the oxygens are removed. It is metallic at $2.75 < x < 3$, but semiconducting for $2.50 < x < 2.65$.[4] For $x = 2.6$, it shows ferromagnetic ordering with 1.7 μ_B/Ni below 230 K[4] and magnetic behavior of the $x = 2.7$ material has been interpreted in terms of a model of ferromagnetic clusters.[5] At $x = 2.5$, where formally the Ni is divalent, a perovskite-type compound La$_2$Ni$_2$O$_5$ forms in which NiO$_6$ octahedra lie along c axis directed chains and NiO$_4$ square-planar units alternate in the a–b plane. This compound shows antiferromagnetic ordering of the NiO$_6$ units along the c axis but no magnetic ordering of the NiO$_4$ units.[6]

Since LaNiO$_2$ with formally monovalent Ni ions was synthesized by Crespin *et al.*[7,8] it has attracted interest[9–11] because it is isostructural to CaCuO$_2$,[12] the parent "infinite layer" material of high T_c superconductors, and like CaCuO$_2$ has a formal d^9 ion among closed ionic shells. However, it is difficult to synthesize and was not revisited experimentally until recently by Hayward *et al.* who produced it as the major phase by oxygen deintercalation from LaNiO$_3$.[13] Their materials consist of two phases, the majority being the infinite-layer (NiO$_2$–La–NiO$_2$) structure and the minority being a disordered derivative phase. Magnetization and neutron powder diffraction reveal no long-range magnetic order in their materials. Its paramagnetic susceptibility has been fit by a Curie–Weiss form in the $150 < T/K < 300$ range with $S = \frac{1}{2}$ and Weiss constant $\theta = -257$ K, but its low T behavior varies strongly from this form. More recently, this same group has produced the isostructural and isovalent nickelate NdNiO$_2$.[14]

One of the most striking features of LaNiO$_2$ is that it potentially provides a structurally simple example of a *monovalent open shell transition metal d^9 ion*. Except for the divalent Cu^{2+} ion, the d^9 configuration is practically nonexistent in ionic solids. In particular, the formal similarity of Ni^{1+} and Cu^{2+} suggests that Ni^{1+} compounds might provide a platform for additional high temperature superconductors. It is these and related questions that we address here.

In this paper we present results of theoretical studies of the electronic and magnetic structures of LaNiO$_2$, and compare with the case of CaCuO$_2$ (or isovalent Ca$_{1-x}$Sr$_x$CuO$_2$) which is well characterized. A central question in transition metal oxides is the role of correlation effects, which are certainly not known *a priori* in LaNiO$_2$ as there is little characterization of the existing material. We look at results both from the local density approximation (LDA) and its magnetic generalization, and then apply also the LDA+U correlated electron band theory that accounts in a self-consistent mean-field way for Hubbard-like intra-atomic repulsion characterized by the Coulomb repulsion U. Our results reveal very different behavior between LaNiO$_2$ and CaCuO$_2$, in spite of the structural and formal d^9 charge similarities. The differences can be traced to (1) the difference in $3d$ site energy between Ni and Cu relative to that of Cu, (2) the ionic charge difference between Ca^{2+} and La^{3+} and associated Madelung potential shifts, and (3) the participation of cation $5d$ states in LaNiO$_2$.

We also discuss briefly our discovery of anomalous behavior in the transition metal $3d^9$ ion as described by LDA+U at large U. Although well beyond the physical range of U for LaNiO$_2$, we find that LDA+U produces what might be characterized as a d^8 "singlet" ion in which the internal configuration is one $d(x^2-y^2)$ hole with spin up and one $d(3z^2-r^2)$ hole with spin down, corresponding to an extreme spin-density anisotropy on the transition metal ion but (nearly) vanishing net moment.
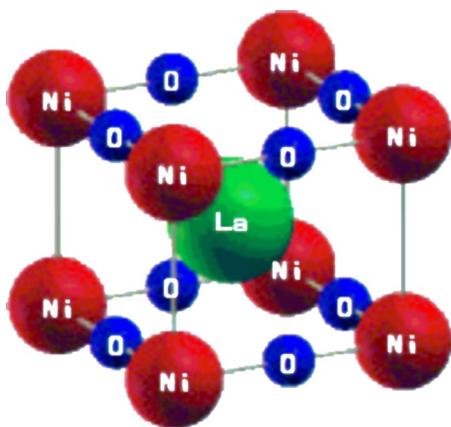
FIG. 1. (Color online) Crystal structure of LaNiO$_2$, isostructural to CaCuO$_2$. Ni ions are in the origin and La ions in the center of the unit cell. It has no axial oxygens.

II. STRUCTURE AND CALCULATION

In the samples of LaNiO$_2$ synthesized and reported by Hayward *et al.*, there exist two phases with space group $P4/mmm$ (No. 123) but different site symmetry.[13] We focus on the majority infinite-layer phase, which is isostructural with CaCuO$_2$.[12] In the crystal structure shown in Fig. 1, Ni ions are at the corners of the square and La ions lie at the center of unit cell. The bond length of Ni–O is 1.979 Å, about 2% more than that of Cu–O in CaCuO$_2$ (1.93 Å). We used the lattice constants $a=3.870\,93$ Å, $c=3.3745$ Å,[13] with a ($\sqrt{2}\times\sqrt{2}$) supercell space group $I4/mmm$ (No. 139) for AFM calculations.

The calculations were carried out with the full-potential nonorthogonal local-orbital (FPLO) method[15] and a regular mesh containing 196 **k** points in the irreducible wedge of the Brillouin zone. Valence orbitals for the basis set were La $3s3p3d4s4p4d5s5p6s6p5d4f$, Ni $3s3p4s4p3d$, O $2s2p3s3p3d$. As frequently done when studying transition metal oxides, we have tried both of the popular forms of functional[16,17] of LDA+U method[18] with a wide range of on-site Coulomb interaction U from 1 to 8 eV, but the intra-atomic exchange integral $J=1$ eV was left unchanged.

For CaCuO$_2$, we used the same conditions as the previous calculation done by Eschrig *et al.* using FPLO.[19]

III. RESULTS

A. LDA Results

We present the LDA results. The paramagnetic (PM) band structure with its energy scale relative to the Fermi energy E_F is given in Fig. 2. A complex of La $4f$ bands is located at +2.5 eV with bandwidth less than 1 eV. The O $2p$ bands extend from about -8 to -3.2 eV. The Ni $3d$ bands are distributed from -3 to 2 eV, with the localized t_{2g} complex near -1.5 eV, while the broad La $5d$ states range from -0.2 to 8 eV. Unlike in PM CaCuO$_2$, there are two bands crossing E_F. One is like the canonical $d(x^2-y^2)$ derived band in the cuprates, rather broad due to the strong $dp\sigma$ antibonding interaction with oxygen p_x, p_y states and enclosing holes centered at the M point. The other band, lying at -0.2 eV at Γ and also having its maximum at the $M=\left(\frac{\pi}{a},\frac{\pi}{a},0\right)$ point, is a mixture of La $5d(3z^2-r^2)$ states and some Ni $3d(3z^2-r^2)$ character. Already this band indicates importance of Ni $3d$–La $5d$ band mixing.

Using a simple one-band tight binding model:

$$\varepsilon_k = \varepsilon_0 - \sum_R t_R e^{i\vec{k}\cdot\vec{R}},$$

the Ni $3d(x^2-y^2)$ band shown in Fig. 3 can be reproduced with a few hopping amplitudes, but requiring more than might have been anticipated. The site energy is $\varepsilon_\circ=93$ meV, slightly above the Fermi level, and the hopping integrals (in meV) are $t(100)=381$, $t(110)=-81$, $t(001)=58$, and $t(111)=-14$. There is no hopping along the (101) direction. As anticipated from the cuprates, the largest hopping is via $t(100)$. However, to correctly describe the k_z dispersion from $X–R$ (i.e., along $\pi/a,0,k_z$) together with the *lack of dispersion* from $\Gamma–Z$ $(0,0,k_z)$ and also $M–A$ $(\pi/a,\pi/a,k_z)$, the third neighbor hopping terms $t(111)$ must be included.

The comparison of the single band tight binding parameters with those of CaCuO$_2$ is given in Table I. It should be noted that the state in mind is an x^2-y^2 symmetry state that is orthogonal to those on neighboring Ni/Cu ions, i.e., an
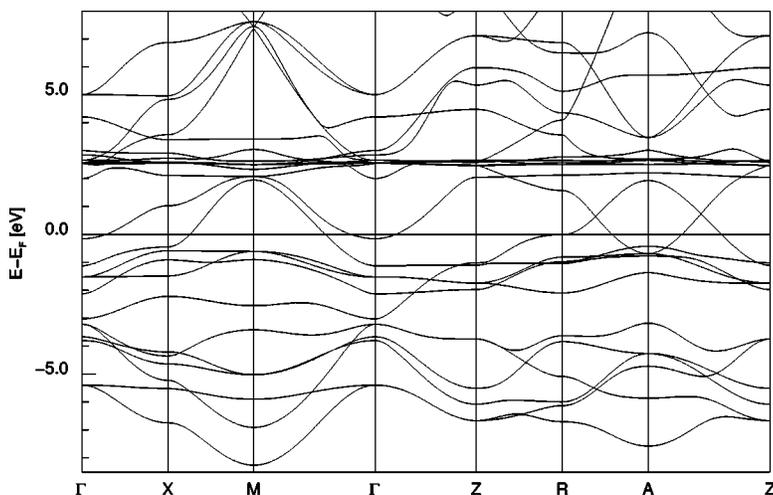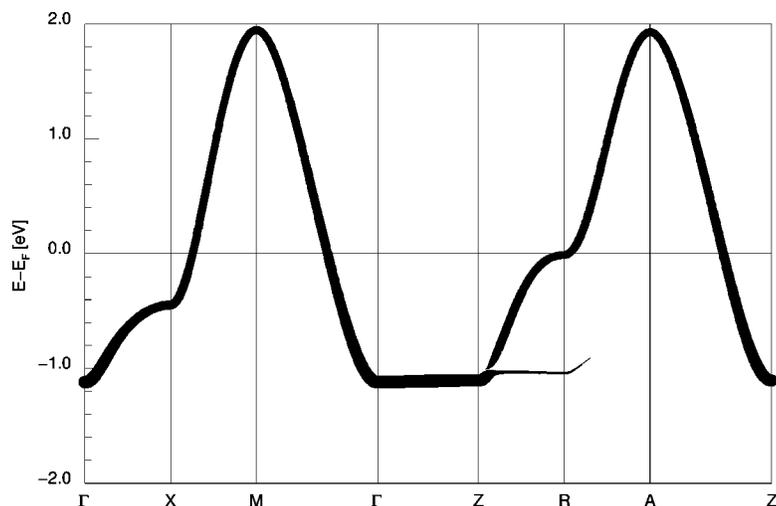

FIG. 2. LDA paramagnetic band structure of LaNiO$_2$. The Ni $3d(x^2-y^2)$ band crosses the Fermi level (zero energy) very much as occurs in cuprates (see Fig. 3). The La $4f$ bands lie on 2.5–3.0 eV. The La $5d(3z^2-r^2)$ band drops below E_F at Γ and A.

FIG. 3. "Fatband" representation of Ni $3d(x^2-y^2)$ in LDA. This band appears at first very two-dimensional, but is not because (1) the saddle point at $X(0,\pi/a,0)$ is not midway between the Γ and $M(\pi/a,\pi/a,0)$ energies, and (2) k_z dispersion between the X and $R(0,\pi/a,\pi/c)$. The dispersions along the $X-R$ and $M-A$ lines (not shown in this figure) are simple cosine-like and dispersionless, respectively.

x^2-y^2 symmetry Wannier orbital. In Ni, the on-site energy is 0.3 eV above what it is in CaCuO$_2$, lying above E_F rather than below. This difference is partially due to the different Madelung potential in the two differently charged compounds, but it also reflects some intrinsic hole doping in the nickelate that leads to a lower Fermi level. The largest hopping amplitude (the conventional t) is 71% of its value in the cuprate, while the second (t') is essentially the same. The $t(001) \equiv t_z$ is also 70% of its value in the cuprate, while the other amplitudes are the almost unchanged.

The LDA Fermi surfaces are shown in Fig. 4. As for the cuprates, the Fermi surface is dominated by the M-centered hole barrel. In this system neighboring barrels touch at $R = (\pi/a, 0, \pi/c)$ because the saddle point at R happens to lie at E_F. The Fermi surfaces also include two spheres containing electrons. The sphere at Γ, with mixed Ni and La $d(3z^2-r^2)$ character, contains about 0.02 electrons. The A-centered sphere is mainly Ni $d(zx)$ in character and contains ~ 0.07 electrons per Ni. The barrel, whose radius of $0.8\pi/a$ in the $(1,1,k_z)$ direction is almost independent of k_z but which varies along $(1,0,k_z)$, possesses about 1.1 holes, accounting for the total of the 1.0 hole that is required by Luttinger's theorem and also fits the formal Ni^{1+} valence (which, being a metal and also mixing with La as well as with O states, is not very relevant).

To investigate magnetic tendencies, attempts to find both ferromagnetic (FM) and antiferromagnetic (AFM) states

TABLE I. Tight binding parameters (in meV) for Ni $3d(x^2-y^2)$ of LaNiO$_2$ and Cu $3d(x^2-y^2)$ of CaCuO$_2$. ε_0 is the site energy and t's are hopping integrals. Ratio (in %) is hopping integrals for LaNiO$_2$ to those for CaCuO$_2$.

Parameters	LaNiO$_2$	CaCuO$_2$	|Ratio| (%)
ε_0	93	-200	
$t(100)$	381	534	71
$t(110)$	-81	-84	96
$t(001)$	58	83	70
$t(101)$	0	-2	0
$t(111)$	-14	-19	74

were made. A stable $\sqrt{2} \times \sqrt{2}$ AFM state, whose band structure is shown in Fig. 5, was obtained, with spin moment 0.53 μ_B per Ni. This state has lower energy by 13 meV/Ni than that of PM state. This is a very small energy difference for this size of moment, suggesting the energy versus moment curve is very flat. Just as for the paramagnetic case, the AFM state has entangled bands of La 5d, Ni 3d, and O 2p character near the Fermi energy. In contrast to the unpolarized case (and CaCuO$_2$), with AFM order the large electron pocket has primarily La $5d(xy)$ character and the slightly occupied electron pocket at Γ has a combination of La $5d(3z^2-r^2)$ and Ni $3d(3z^2-r^2)$ character. Attempts to obtain a FM solution always led to a vanishing moment.

The strong difference between CaCuO$_2$ and LaNiO$_2$ is therefore already evident from the LDA results as well as from the experimental data. CaCuO$_2$ is strongly AFM, a result which LDA entirely fails to predict, and only nonmagnetic solutions are found. LaNiO$_2$ shows no magnetism, whereas LDA finds the antiferromagnetically ordered state is lower in energy (albeit by a small amount). The differences
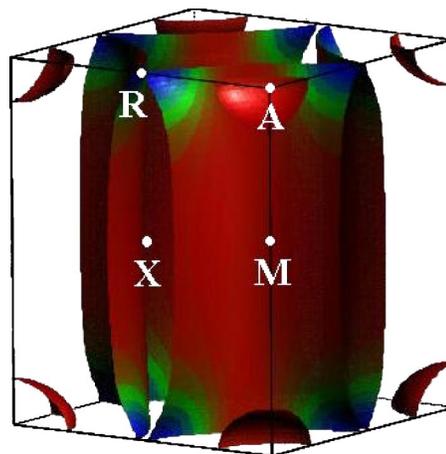

FIG. 4. (Color online) Paramagnetic Fermi surface in the local density approximation. In the center (not visible), i.e., Γ, there is a sphere [a radius $0.25(\pi/a)$] having $d(3z^2-r^2)$ character of Ni and La. The cylinder with radius $0.8(\pi/a)$ contains Ni $d(x^2-y^2)$ holes, whereas another sphere [a radius $0.4(\pi/a)$] at each corner contains Ni $d(zx)$ electrons.
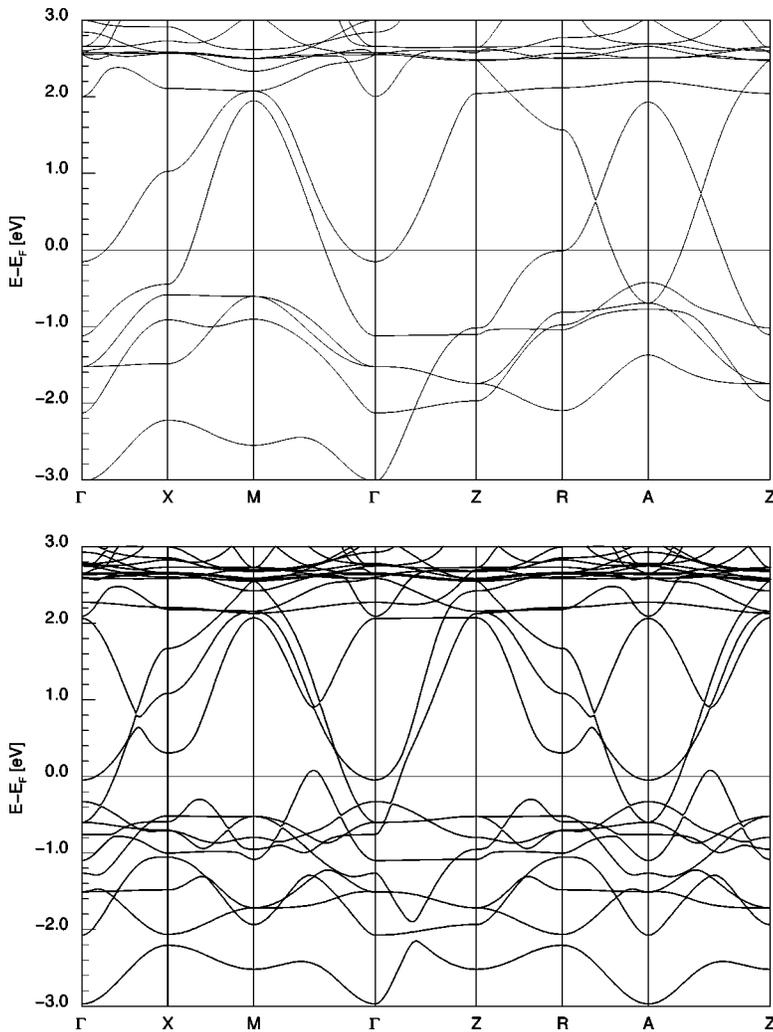
FIG. 5. LDA band structures of LaNiO$_2$, graphed on the same energy scale. Top panel: paramagnetic; bottom panel: antiferromagnetic. The Ni 3d bands lie above -3 eV and are disjointed from the O 2p bands (not shown) which begin just below -3 eV. The antiferromagnetism introduces the gap in the Ni $dp\sigma$ band midway between Γ and M in the range 0–1 eV. The symmetry points are given such as $(0,0,x)$ for $\Gamma(Z)$, $(1/2,1/2,x)$ for $X(R)$ and $(1,0,x)$ for $M(A)$. x is zero for the first symbols and 1 for the symbols in parentheses.

between these two systems also are highlighted in the following sections.

B. Consideration of correlation with LDA+U

As noted in Sec. I, no magnetic order has been observed in LaNiO$_2$, either by magnetization or by neutron scattering. Although the local density approximation often does quite well in predicting magnetic moments, for weakly or nearly magnetic systems renormalization by spin fluctuations becomes important[20–22] and such effects are not included in the local density approximation. The small energy difference in energy between the AFM and nonmagnetic solutions indicates the error is in some sense small.

There is still the unsettled question of the strength of correlation effects due to an intra-atomic repulsion U on the Ni site. For example, there is not yet any specific heat data to show whether the carrier mass is enhanced or not. Making the analogy to CaCuO$_2$ (same formal d^9 configuration, same structure, neighboring ion in the periodic table), which is a strong antiferromagnetic insulator, suggests that effects due to U might have some importance. As we have noted above, this analogy seems to be rather weak. Here we apply the LDA+U "correlated band theory" method to assess effects

of intra-atomic repulsion and compare with observed behavior. In Sec. IV we compare and contrast with CaCuO$_2$.

Upon increasing U from zero in the antiferromagnetically ordered phase, the spin magnetic moment of Ni increases from the LDA value of 0.53 μ_B to a maximum of 0.8 μ_B at $U=3$ eV. Surprisingly, for $U>4$ eV the moment steadily decreases and by $U=8$ eV it has *dropped* to 0.2 μ_B/Ni, which is less than half of its LDA value, as shown in Fig. 6. We emphasize that this behavior is unrelated to the observed behavior of LaNiO$_2$ (which is nonmagnetic). However, this unprecedented response of the transition metal ion to the imposition of a large U gives new insight into a feature of the LDA+U method that has not been observed previously. We now relate some details of the results that are intended to enhance our understanding of the LDA+U method in materials such as these; the remainder of this subsection is probably irrelevant to the interpretation of data on LaNiO$_2$.

This "quenching" of the local moment with increasing U results from behavior of Ni $3d(3z^2-r^2)$ states that is analogous to those of the $3d(x^2-y^2)$, but with the direction of spin inverted (then with additional complications). As usual for a d^9 ion in this environment, the majority $3d(x^2-y^2)$ state of Ni is fully occupied even at $U=2$ eV, while the minority state is completely unoccupied at $U=3$ eV, where the moment is
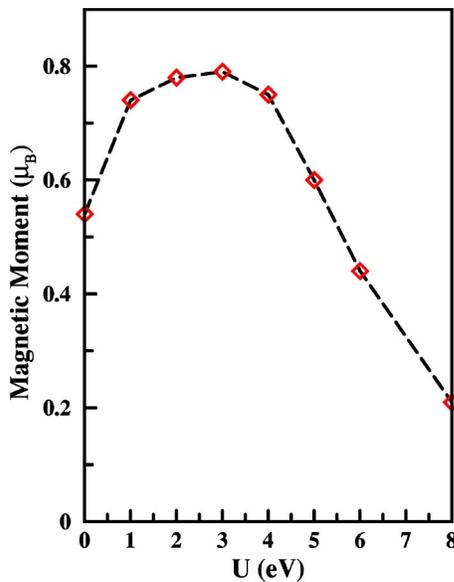
FIG. 6. Behavior of the Ni magnetic moment vs the interaction strength U in antiferromagnetic LaNiO$_2$.

FIG. 8. Isocontour plot of the spin density of the "singlet" Ni ion ($U=8$ eV) when there is an x^2-y^2 hole with spin up and a $3z^2-r^2$ hole with spin down. Dark and light surfaces denote isocontours of equal magnitude but opposite sign.

maximum and the system is essentially Ni^{1+} $S=\frac{1}{2}$. One can characterize this situation as a Mott insulating $3d(x^2-y^2)$ orbital, as in the undoped cuprates. At $U=3$ eV, the density of states has a quasi-one-dimensional van Hove singularity due to a flat band just below (bordering) the Fermi energy as can be seen in the $3d$ DOS shown in Fig. 7. Upon increasing U to 4 eV, rather than reinforcing the $S=\frac{1}{2}$ configuration of Ni and thereby forcing the La and O ions to cope with electron/hole doping, the Ni $d(3z^2-r^2)$ states begin to polarize. The charge on the Ni ion drops somewhat, moving it in the Ni$^{1+}\rightarrow$Ni^{2+} direction, with the charge going into the La $5d$–O $2p$ states. Idealizing a bit, one might characterize the movement of (unoccupied) majority character of $3d(3z^2-r^2)$ well above E_F as a Mott transition of these orbitals, which is not only distinct from that of the $3d(x^2-y^2)$
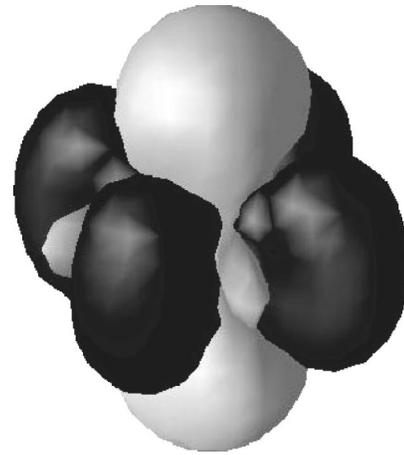
states, but is oppositely directed, leading to an on-site "singlet" type of cancellation.

This movement of states with increasing U has been emphasized in Fig. 7 for easier visualization. The resulting spin density on the transition metal ion at $U=8$ eV is pictured in Fig. 8. There is strong polarization in all directions from the core except for the position of nodes. The polarization is strongly positive (majority) in the lobes of the $3d(x^2-y^2)$ orbital, and just as strongly negative (minority spin) in the lobes of the $3d(3z^2-r^2)$ orbital. The net moment is (nearly) vanishing, but this results from a singlet combination (as nearly as it can be represented within classical spin picture) of spin-half up in one orbital and spin-half down in another orbital that violates Hund's first rule. The magnetization density is large throughout the ion, but integrates to (nearly) zero.

This behavior is however more complicated than a Mott splitting of occupied and unoccupied state, as can be seen
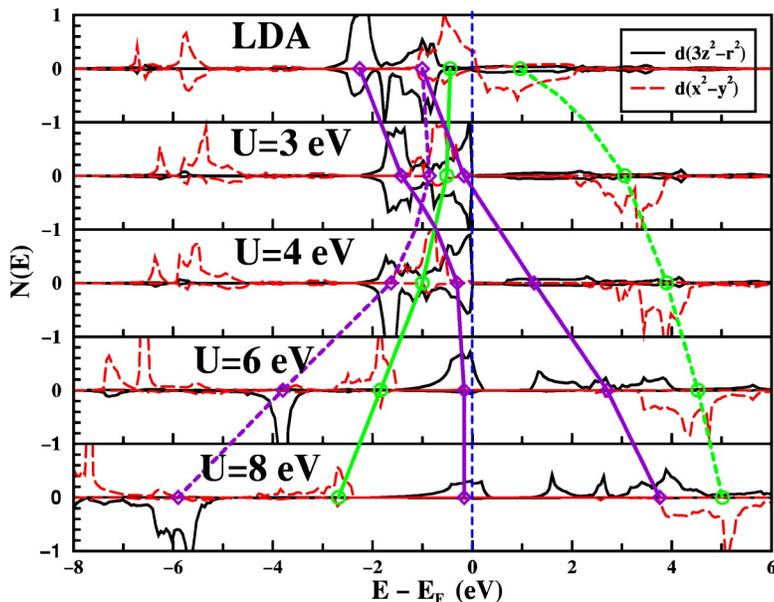

FIG. 7. (Color online) Change of the Ni $3d(3z^2-r^2)$ and $3d(x^2-y^2)$ densities of states as on-site Coulomb interaction U increases. One can easily identify a splitting ("Mott transition") of the $3d(x^2-y^2)$ states occurring near $U=0$, and the light (green) lines outline their path with increasing U (majority is solid, minority is dashed). A distinct Mott transition involving oppositely directed moment of the $3d(3z^2-r^2)$ states is outlined with the dark (purple) lines. This moment is oppositely directed. The conceptual picture is also complicated by the splitting even at $U=0$ which persists in the majority states, leaving a band at E_F with strong Ni $3d(3z^2-r^2)$ character as well as the expected upper Hubbard band at 4 eV.

from the substantial Ni $3d$ character that remains, even for $U=8$ eV, in a band straddling E_F while the rest of the weight moves to ~4 eV. In both of these bands there is strong mixing with La $5d(xy)$ states. What happens is that as the "upper Hubbard $3d(3z^2−r^2)$ band" rises as U is increased, it progressively mixes more strongly with the La $5d(xy)$ states, forming a bonding band and an antibonding band. While the antibonding combination continues to move upward with increasing U, the bonding combination forms a half-filled band which remains at E_F.

Thus we have found that for the Ni^{1+} ion in this environment, increasing U (well beyond what is physically plausible for LaNiO$_2$) results in $S=\frac{1}{2}$ Ni^{+1} being converted into a nominal Ni^{+2} ion (the actual charge changes little, however) in which the two holes are coupled into an intra-atomic $S=0$ singlet. This behavior involves yet a new kind of correlation between the $3d(3z^2−r^2)$ states and the $3d(x^2−y^2)$ states, but one which is due to (driven by) the local environment.

This behavior is quite different from the results for $U=8$ eV reported by Anisimov, Bukhvalov, and Rice[10] using the Stuttgart TBLMTO-47 code. They obtained an AFM insulating solution analogous to that obtained for CaCuO$_2$,[19] with a single hole in the $3d$ shell occupying the $3d(x^2−y^2)$ orbital that antibonds with the neighboring oxygen $2p_\sigma$ orbital. The reason for this difference is not clear. Their code makes shape restriction on density and potential that are relaxed in our code, it appears that La $4f$ states were not included, and the LDA+U functional form was not strictly identical to what we have used, but we do not expect any of these differences would be responsible for the difference in solutions. It is established that multiple solutions to the LDA+U equations can occur,[23,24] and we have also found (in other applications) that different starting points can be used to encourage the discovery of alternative solutions. Our attempts to do so have always led only to the solutions given in Fig. 7.

IV. COMPARISON WITH CaCuO$_2$ AND DISCUSSION

Although Ni^{+1} is isoelectronic to Cu^{+2}, both the observed and the calculated behavior of LaNiO$_2$ are very different from CaCuO$_2$. In contrast to CaCuO$_2$, LaNiO$_2$ is (apparently) metallic, with no experimental evidence of magnetic ordering for LaNiO$_2$. The differing electronic and magnetic properties mainly arise from two factors. First, the Ca $3d$ bands lying in the range of 4 and 9 eV are very differently distributed from the broader and lower La $5d$ bands in the range of −0.2 and 8 eV. Second, in CaCuO$_2$, O $2p$ states extend to the Fermi level and overlap strongly with Cu $3d$ states, and the difference of the two centers is less than 1 eV, as can be seen in Fig. 9. Thus, there is a strong $2p−3d$ hybridization that has been heavily discussed in high T_c materials. In LaNiO$_2$, however, Ni $3d$ states lie just below the Fermi level, with O $2p$ states located 3–4 eV below the center of Ni bands. Therefore, p-d hybridization, which plays a crucial role in the electronic structure and superconductivity of CaCuO$_2$, becomes much weaker.

V. SUMMARY

Aside from the formal similarity to CaCuO$_2$, the interest in LaNiO$_2$ lies in the occurrence of the unusual monovalent
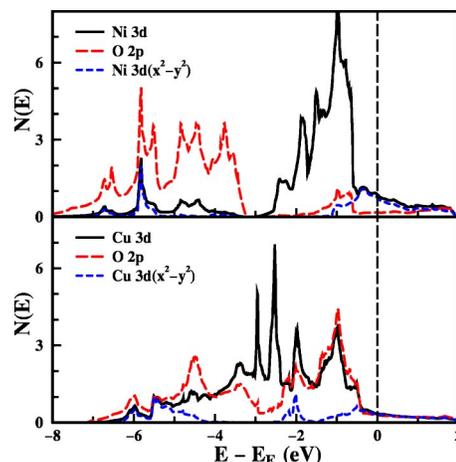

FIG. 9. (Color online) Comparison of LDA projected paramagnetic DOS LaNiO$_2$ (upper panel) and CaCuO$_2$ (lower panel). Note the separation of the Ni $3d$ states from the O $2p$ states in the upper panel, which does not occur for the more strongly hybridized cuprate.

Ni ion. As we have found and in apparent agreement with experiment, this compound is a metal, and the "charge state" of a transition metal atom in a metal usually has much less significance than it is in an insulator. It may be because the compound is metallic that it is stable, but in this study we are not addressing energetics and stability questions.

Hayward et al.[13] had already suggested that the experimental findings could arise from reduced covalency between the Ni $3d$ and O $2p$ orbitals, and the 30% smaller value of the hopping amplitude t reflects the smaller covalency, as does the increased separation between the Ni $3d$ and O $2p$ bands. It is something of an enigma that in CaCuO$_2$ and other cuprates, LDA calculations fail to give the observed antiferromagnetic states, while in LaNiO$_2$ LDA predicts a weak antiferromagnetic state when there is no magnetism observed. In the cuprates the cause is known and is treated in a reasonable way by application of the LDA+U method. In this nickelate, application of the LDA+U method does not seem to be warranted (although behavior occurs it if it used). Rather, the prediction of weak magnetism adds this compound to the small but growing number of systems (ZrZn$_2$,[25] Sc$_3$In,[26] and Ni$_3$Ga,[22] for example) in which the tendency toward magnetism is overestimated by the local density approximation. It appears that this tendency can be corrected by accounting for magnetic fluctuations.[20,22] The isovalent compound NdNiO$_2$ reported by Hayward and Rosseinsky[14] may help to clarify this unusual nickelate system, although its microstructure is not simple and the Nd magnetism will impede the study of the Ni magnetic behavior.

[1] J. B. Goodenough and P. M. Raccah, J. Appl. Phys. **36**, 1031 (1965).

[2] K. Sreedhar, J. M. Honig, M. Darwin, M. McElfresh, P. M. Shand, J. Xu, B. C. Crooker, and J. Spalek, Phys. Rev. B **46**, 6382 (1992).

[3] N. Gayathri, A. K. Raychaudhuri, X. Q. Xu, J. L. Peng, and R. L. Greene, J. Phys.: Condens. Matter **10**, 1323 (1998).

[4] T. Moriga, O. Usaka, I. Nakabayashi, T. Kinouchi, S. Kikkawa, and F. Kanamaru, Solid State Ionics **79**, 252 (1995).

[5] Y. Okajima, K. Kohn, and K. Siratori, J. Magn. Magn. Mater. **140–144**, 2149 (1995).

[6] J. A. Alonso, M. J. Martínez-Lope, J. L. García-Muñoz, and M. T. Fernández-Díaz, J. Phys.: Condens. Matter **9**, 6417 (1997).

[7] M. Crespin, P. Levitz, and L. Gatineau, J. Chem. Soc., Faraday Trans. 2 **79**, 1181 (1983).

[8] P. Levitz, M. Crespin, and L. Gatineau, J. Chem. Soc., Faraday Trans. 2 **79**, 1195 (1983).

[9] J. Choisnet, R. A. Evarestov, I. I. Tupitsyn, and V. A. Veryazov, J. Phys. Chem. Solids **57**, 1839 (1996).

[10] V. I. Anisimov, D. Bukhvalov, and T. M. Rice, Phys. Rev. B **59**, 7901 (1999).

[11] M. J. Martínez-Lope, M. T. Casais, and J. A. Alonso, J. Alloys Compd. **275–277**, 109 (1998).

[12] T. Siegrist, S. M. Zahurak, D. W. Murphy, and R. S. Roth, Nature (London) **334**, 231 (1998).

[13] M. A. Hayward, M. A. Green, M. J. Rosseinsky, and J. Sloan, J. Am. Chem. Soc. **121**, 8843 (1999).

[14] M. A. Hayward and M. J. Rosseinsky, Solid State Sci. **5**, 839 (2003).

[15] K. Koepernik and H. Eschrig, Phys. Rev. B **59**, 1743 (1999).

[16] M. T. Czyzyk and G. A. Sawatzky, Phys. Rev. B **49**, 14211 (1994).

[17] V. I. Anisimov, I. V. Solovyev, M. A. Korotin, M. T. Czyzyk, and G. A. Sawatzky, Phys. Rev. B **48**, 16929 (1993).

[18] V. I. Anisimov, J. Zaanen, and O. K. Andersen, Phys. Rev. B **44**, 943 (1991).

[19] H. Eschrig, K. Koepernik, and I. Chaplygin, J. Solid State Chem. **176**, 482 (2003).

[20] T. Moriya, *Spin Fluctuations in Itinerant Electron Magnetism* (Spinger, Berlin, 1985).

[21] I. I. Mazin, D. J. Singh, and A. Aguayo, in Proceedings of the NATO ARW on *Physics of Spin in Solids: Materials, Methods, and Applications*, edited by S. Halilov (Kluwer, New York, 2004); cond-mat/0401563.

[22] A. Aguayo, I. I. Mazin, and D. J. Singh, Phys. Rev. Lett. **92**, 147201 (2004).

[23] A. B. Shick, W. E. Pickett, and A. I. Liechtenstein, J. Electron Spectrosc. Relat. Phenom. **114–116**, 753 (2001).

[24] A. B. Shick, V. Janis, V. Drchal, and W. E. Pickett, Phys. Rev. B **70**, 134506 (2004).

[25] D. J. Singh and I. I. Mazin, Phys. Rev. B **69**, 020402 (2004).

[26] A. Aguayo and D. J. Singh, Phys. Rev. B **66**, 020401 (2002).